SCIENTIFIC REPORTS

OPEN

Novel triadius-like N_4 specie of iron nitride compounds under high pressure

Received: 11 May 2018
Accepted: 2 July 2018
Published online: 13 July 2018

Yuanzheng Chen[1], Xinyong Cai[1], Hongyan Wang[1], Hongbo Wang[2] & Hui Wang[2]

Various nitrogen species in nitrides are fascinating since they often appear with these nitride as superconductors, hard materials, and high-energy density. As a typical complex, though iron nitride has been intensively studied, nitrogen species in the iron–nitrogen (Fe-N) compounds only have been confined to single atom (N) or molecule nitrogen (N_2). Using a structure search method based on the CALYPSO methodology, unexpectedly, we here revealed two new stable high pressure (HP) states at 1:2 and 1:4 compositions with striking nitrogen species. The results show that the proposed FeN_2 stabilizes by a break up of molecule N_2 into a novel planar N_4 unit (*P6*$_3$*/mcm*, >228 GPa) while FeN_4 stabilizes by a infinite 1D linear nitrogen chains N∞ (*P*-1, >50 *GPa*; *Cmmm*, >250 GPa). In the intriguing N_4 specie of *P6*$_3$*/mcm*-FeN_2, we find that it possesses three equal N = N covalent bonds and forms a perfect triadius-like configuration being never reported before. This uniqueness gives rise to a set of remarkable properties for the crystal phase: it is identified to have a good mechanical property and a potential for phonon-mediated superconductivity with a T_c of 4–8 K. This discovery puts the Fe-N system into a new class of desirable materials combining advanced mechanical properties and superconductivity.

Nitrogen (N) is the most abundant element in the earth's atmosphere and is one of the least studied elements regarding the composition of the Earth[1]. At standard temperature and pressure (T = 298 K; P = 1 atm), elemental nitrogen is a gas, consisting of diatomic N_2 molecules that are bound by stiff covalent triple bonds. So the molecule is chemically inert and hardly dissociate and not many higher molecular or extended structures are known for nitrogen other than N_2 under normal conditions. Syntheses of useful nitrides with various nitrogen species rely on chemical methods via, e.g., photochemical reaction, electrochemical synthesis[2–8]. A few higher molecular units are known, such as photolytic cyclic N_3[3,4], the tetrahedral N_4 molecule[5], the N_5^- anion[6], and the N_5^+ in a crystalline phase of $N_5^+SbF_6^-$[7,8]. Note that, among these units, though the tetrahedral N_4 has been a form of the N_4 unit for synthesis, it is observed as a metastable species with a lifetime exceeding one microsecond.

Besides the chemical methods, in fact, adopting HP technology nitrogen also does form innumerable stable and metastable chemical compounds with various nitrogen species[9–17]. These nitrogen species have various structural forms ranging from single atom (N) to molecular (N_2, N_3, N_4, N_5, N_6) units and polynitrides[13–17]. To note, these stable nitrides have a variety of intriguing properties, such as superconductivity (MoN)[13], high-energy density (LiN_3, NaN_3)[14], and high hardness (WN_2)[15], as well as extraordinary chemical and thermal stability (Xe-N)[16]. These nitrides aroused our significant interest in the field of exploring new HP nitrogen species and their potential remarkable properties.

As a typical transition-metal nitride, the Fe-N system is extensively investigated to explore its compounds in the interior layers of earth following its first discovery since 19 century[2]. A rich Fe-N chemistry exists, most synthesized compounds have a Fe/N ratio higher than unity, such as α''-$Fe_{16}N_2$, α'-Fe_8N, γ'-Fe_4N, Fe_7N_3, Fe_3N_x(x = 0.75–1.4), Fe_3N, Fe_2N and FeN[4–10]. Among, the FeN compound is most nitrogen-rich iron nitride reported benign synthesized in a high pressure apparatus thus far[10]. This synthesis of FeN spurred the endeavors in search for Fe-N compounds with a more nitrogen content exceeding the FeN compound with other nitrogen species. However, in contrast to the Fe-rich compounds, there is little work on the N-rich iron nitrides, both from the experimental and theoretical sides. Only few theoretical investigations are available to report that an N-rich

[1]School of Physical Science and Technology, Key Laboratory of Advanced Technologies of Materials, Ministry of Education of China, Southwest Jiaotong University, Chengdu, 610031, China. [2]State Key Lab of Superhard Materials, Jilin University, Changchun, 130012, China. Correspondence and requests for materials should be addressed to Y.C. (email: cyz@calypso.org.cn) or Hongbo W. (email: cyz@home.swjtu.edu.cn)

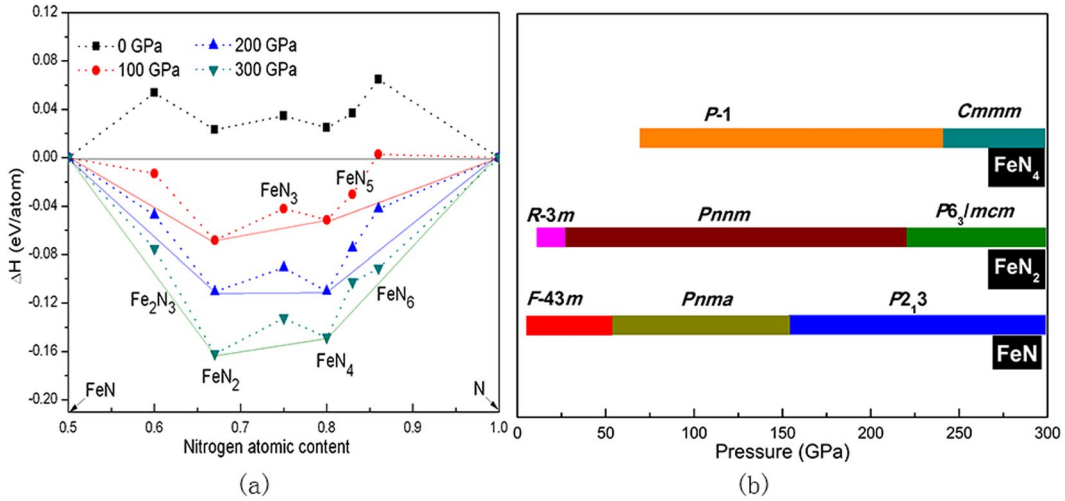

Figure 1. (**a**) Formation enthalpies (ΔH) of various Fe-N compounds with respect to decomposition into constituent elemental solids at 0–300 GPa. Data points located on the convex hull (solid lines) represent stable species against any type of decomposition. (**b**) Pressure ranges in which the corresponding structures of FeN, FeN_2 and FeN_4 are stabilized.

iron pernitride (FeN_2) crystallizes in the space group *R*-3*m* at 17 GPa (1000 K)[11] and transforms an orthorhombic *Pnnm* structure up to 22 GPa[12] obtained by assuming the parent metal under pressure. All these known Fe–N compounds adapt single N atom or molecule N_2 configuration and keep iron 6-coordination.

In order to systematically explore the possibility of obtaining new stable N-rich iron nitrides, and especially to examine the possibility of attaining new nitrogen species at HP, we here present extensive structure searches of stoichiometric Fe-N compounds under various pressures ranging from 0 to 300 GPa, using an unbiased particle swarm optimization (PSO) algorithms for crystal structure predictions[18]. This swarm-intelligence high-throughput searching has proven effective in revealing new compositions favorable to form in large sets of multicomponent Ca-H, Li-B, Xe-N, Cs-N systems[16,17,19,20]. The effectiveness has been also demonstrated by recent successes in predicting high-pressure structures of various systems, and their several experimental confirmations[21–30]. In this work, we proposed new N-rich iron nitrides at 1:4 and 1:2 compositions under HP. Identifying their nitrogen species, it is strikingly found that the nitrogen species evolve from a N_2 unit to a novel N_4 units, and eventually N∞ with the increase of N contents. In N_4 unit, we find that it possesses three N = N covalent bonds and one lone pair, which leads it to forms an unknown triadius-like configuration. Its structural uniqueness gives rise to a set of remarkable properties for the crystal $P6_3/mcm$ phase with an unexpectedly Tc of 4~8 K and a good mechanical property.

Methods

The developed CALYPSO structure prediction method designed to search for the stable structures of given compounds has been employed for the investigation of phase stability of Fe-N systems in N-rich stoichiometry under HP. We performed structure predictions of stoichiometric $Fe_{1-i}N_i$ ($0 < i < 1$) with simulation cell sizes of 1–4 formula units (f.u.) in a pressure range from 0 to 300 GPa. The local structural relaxations and electronic band structure calculations were performed in the framework of density functional theory within the generalized gradient approximation (GGA) and frozen-core all-electron projector-augmented wave (PAW) method[31,32], as implemented in the VASP code[33]. The PAW pseudopotentials with $3d^7 4s^1$ and $2s^2 2p^3$ valence electrons were adopted for Fe and N, respectively. The kinetic energy cutoff for the plane-wave basis set is taken as 800 eV and a dense k-point grid with the spacing of $2\pi \times 0.03$ Å^{-1} was used to sample the Brillouin zone, which was shown to yield excellent convergence for total energies (within 1 meV/atom). The phonon calculations were carried out by using a finite displacement approach through the PHONOPY code[34]. The electron-phonon coupling (EPC) of $P6_3/mcm$-FeN_2 was calculated within the framework of linear response theory through the Quantum-ESPRESSO code[35]. A $2 \times 2 \times 2$ q mesh was used in the interpolation of the force constants for the phonon dispersion curve calculations. A MP grid of $12 \times 12 \times 12$ was used to ensure k-point sampling convergence, which approximates the zero-width limits in the calculations of EPC parameter. We Elastic constants were calculated by the strain-stress method and the bulk modulus and shear modulus were thus derived from the Voigt-Reuss-Hill averaging scheme[36].

Results and Discussions

We focused our structure search on the phase stabilities of Fe-N systems in N-rich stoichiometry by calculating the formation enthalpy of various $Fe_{1-i}N_i$ ($0 < i < 1$) compounds in a pressure range of 0 to 300 GPa. The formation enthalpy was calculated with respect to the decomposition into FeN and N, as $\Delta h(Fe_{1-i}N_i) = h(Fe_{1-i}N_i) - (1-i)h(FeN) - (2i-1)h(N)$, where the enthalpies h for $Fe_{1-i}N_i$ and FeN are obtained for the most stable structures as searched by the CALYPSO method at the desired pressures. The convex hulls are depicted in Fig. 1a for pressures at 0, 100, 200 and 300 GPa. The validity of using FeN instead of Fe in defining Δh is ensured by the fact that

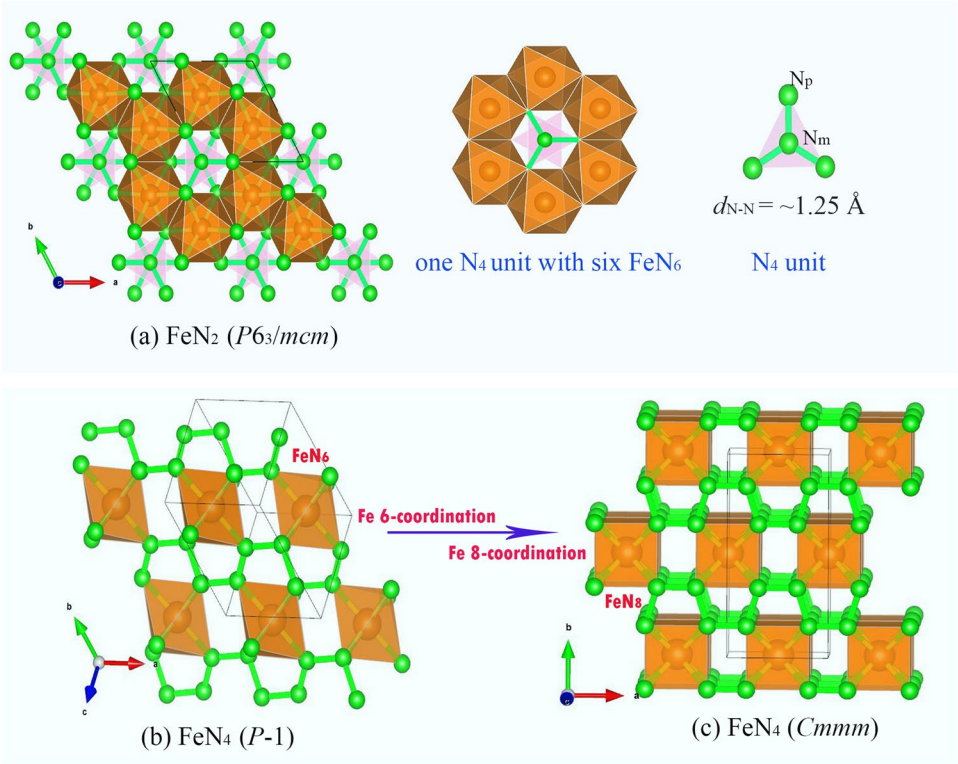

Figure 2. Structures of predicted stable FeN_2 and FeN_4 crystals: (**a**) The $P6_3/mcm$ structure of FeN_2, viewing of the FeN_6 and N_4 unit. (**b**) Low pressure P-1 structure of FeN_4. (**b**) the HP $Cmmm$-FeN_4.

FeN is exceedingly stable with respect to the binary Fe-N system having a max nitrogen ratio below 50% (Fe_4N, Fe_3N, Fe_2N) under HP, as revealed by our study (Fig. S1) and relative experimental studies[4–7,10]. The stable structure of FeN below 50 GPa has space group F-43m structure (Fig. S2, ref.[10]). At 50 GPa, the FeN transforms into a *Pnma* structure (Fig. S3), followed by a cubic $P2_13$ structure above 150 GPa (Fig. S4). All these FeN structures takes on isolated N atomic sublattice and keeps six-fold coordinated by Fe forming edge-sharing FeN_6 octahedron in their corresponding stable pressure ranges.

Magnetism plays a central role in iron and its compounds. Therefore it is necessary to confirm the role of magnetism on the stability of these Fe-N structures. From our spin-polarized calculations, we find that every Fe atom of Fe-N compounds possesses a magnetic moment of 0.21–1.68 μ_B under pressure (<50 GPa), which is substantially lower than that of the pure Fe solid (2.2 μ_B). Meanwhile, the magnetic moment will decrease rapidly with increasing pressure and be completely quenched as pressure exceeds 50 GPa. As an example, we performed the energy calculations of FeN after considering magnetism and found that the magnetic effect did not change the phase transition sequence but slightly shifted the phase transition pressure. According to a model derived from a Slater-Pauling type behavior[37], the magnetization with increasing amount of N becomes decrease in the Fe–N system. It thus is plausible to perform the structure search and enthalpy calculations without considering the magnetic effect under HP in the N-rich Fe–N compounds.

Analysis the convex hull for researching the thermodynamically stable in the Fig. 1a, we can get a main result as follows: at $P = 0$ GPa, the Δh of all N-rich stoichiometry are positive, meaning that the nitrogen ratio above 50% Fe-N system are not stable. This is consistent with the experimental observation that no Fe-N compound whose which the nitrogen content exceeds the iron content can form at ambient pressure; at 100 GPa, stable stoichiometries of FeN_2 and FeN_4 emerge on the convex hull as the most stable stoichiometry, this situation preserves up to 300 GPa. Detailed pressure-composition phase diagram for these two N-rich species is presented in Fig. 1b. Moreover, we performed phonon spectra calculations using the finite-displacement method to assess the dynamical structural stability of their structural phases at desired pressure. No imaginary frequency was found for their structures, which indicated that they are dynamically stable (Figs S5–10).

In the FeN_2 compound, the low pressure crystalline phase is a trigonal R-3m structure at approximately 22 GPa, above which an orthorhombic *Pnnm* structure becomes more favorable, consistent with the previous reports[11,12]. These two structures both contain a dinitrogen unit and N-sharing six-fold FeN_6 octahedrons (Figs S11,12). Analysis of the dinitrogen unit indicating a strong N-N covalent bond and the dinitrogen unit can be formulated as $(N\text{-}N)^{2-}$ and $(N=N)^{2-}$ in the R-3m and *Pnnm* structures, respectively[11,12]. Recently, these phases have been synthesized and verified by the experiment under high pressure and high temperature[38]. Upon to 228 GPa, an unknown energetically more favored hexagonal $P6_3/mcm$ structure was firstly discovered (Fig. 2a). Tracing the volume change of the phase transition from *Pnnm* to $P6_3/mcm$, it is found that this transition is a first-order accompanied by a volume drop of 3.5%. Viewing the $P6_3$/mcm structure, it contains two types of N

atoms occupying two different 2*c* Wyckoff sites as middle N_m and peripheral N_p (Fig. 2a): the N_p atom is shared by four Fe atoms forming a FeN_6 octahedron with Fe-N_p distances of 1.76 Å, while the N_m atom bonds with three N_p atoms forming perfect N_4 unit with a bond length of ~1.25 Å (at 300 GPa). These Fe-N_p distances are shorter than the sum (1.92 Å) of covalent radii of Fe and N atoms. In such exotic structure, each Fe forms 6 Fe-N_p bonds with those 6 neighboring N_p atoms and each N_p atom has four neighbors Fe-N_p bonds and a N_p-N_m bond. The N_p-N_m distance (1.25 Å) is slightly longer than the double N = N bonds (1.20 Å) can be verified as the N = N bonding nature.

In the FeN_4 compound, the energetically favored structure of FeN_4 (stable above 50 GPa) has a triclinic structure with a low *P*-1 symmetry (Fig. 2b). The nitrogen sublattice in this structure takes on a polyacetylene-like infinite linear chain structure with a closest NN separation (N∞) in the range of 1.32−1.34 Å. Polyhedral view of the *P*-1 structure, it forms octahedrons linked together by the NN bonds of N∞, with Fe atoms sitting at the center of octahedrons and being 6-fold bonded to the N atoms of N∞. Up to 250 GPa, a surprising transition from such the 6-fold *P*-1 structure to a 8-fold structure takes place. This 8-fold structure adopts a high symmetric orthorhombic *Cmmm* structure, which have similar N∞ structural character of the *P*-1 phase (Fig. 2c). Analysis of their ELF (Figs S15,16) suggests that the N atoms of N∞ are in sp^2 hybridization, each N forms two σ bonds with two neighboring N atoms and one Fe-N bond. Due to the N∞ units, the electronic structures of these two phases both exhibit the metal properties (Figs S17,18). Such N∞ units and electronic properties can be also found in works for LiN_3, NaN_3, and CsN_3 under high pressure[39–41]. For the two phases, their different is that the *Cmmm* phase are composed of a Fe 8-coordination decahedrons, in stark contrast with 6-coordination in the octahedrons of *P*-1 structure (Fig. 2b,c). Analyses of the coordination number of Fe, we note that conventional coordination chemistry of Fe consists of four-, five-, and six-coordinate metal ions, while coordination numbers higher than six are seldom observed in only discrete molecules and polynuclear metal clusters[42–49]. Despite much effort, the Fe atoms are found to be very resistive to become 8-fold coordinate in solids, and the search for solids containing 8-coordinate has so far been scarcely successful. To our knowledge, this is first time to identify the 8-fold coordination of Fe atoms in the Fe-N compounds.

Return to identify the nitrogen species of Fe-N compounds (FeN, FeN_2 and FeN_4), it is strikingly found that the nitrogen sublattice evolve from isolated N atom to in turn the N_2 unit, the N_4 unit and eventually N∞ with the increase of N contents. It is noted that these features, except for the N_4 units, can be often found in alkali metal azides (Li-N, Na-N, Cs-N)[39–41]. Tracing the history of the related N_4 units, the first investigation into N_4 units can be traced back to a reported about successfully isolated neutral N_4 molecule in the gas phase a decade ago[5], but the lifetime of the N_4 molecule is only around 1 microsecond. Recently, a charged N_4 species as predicted in the CsN crystal is substantially stabilized by strong cation-anion interactions[17]. This predicted N_4^{4-} anion has an open-chain structure containing two terminal single-bonds and one internal double-bond. Being different that, we found here the N_4 units of $P6_3/mcm$-FeN_2 has three equal N = N bond and forms plane N_4 units like as the triadius star (Fig. 3a). We also try to look for crystal structures that incorporate such special N_4 units in the other systems. But no crystal structure is found so far. Here the exotic N_4 unit having strong N-N covalent bonding can be clearly shown by its ELF (Fig. 3b,c). Each N_m atom possesses one lone pair of electrons at its p_z orbital and forms three N = N covalent bonds with peripheral N_p (N1, N2, N3) atoms (Fig. 3c), owing to its sp^2 hybridization.

Notice that the p_z orbital of N is much lower in energy than that of Fe and form a strong overlapping between p_z orbitals of N. This fact justifies us to study the electronic structure of hypothetic neutral N_4 unit first before researching the electronic properties of its crystal $P6_3/mcm$ structure. The atomic model for neutral N_4 unit is sketched in Fig. 3d with several typical symmetry elements of point group D_{3h} marked out explicitly (Table S7). The linear combination of three p_z orbitals of peripheral N_p can form orbitals with A_2'' and E'' symmetry, while the p_z orbital of N_m belongs to A_2'' (Table S8). Therefore, for a bare N_4 unit, the four p_z orbitals of N would constitute two nonbonding (E''), one bonding and one antibonding molecular orbitals. According to the diagram in Fig. 3e, the HOMO derives from the nonbonding p_z orbitals of N_p atoms, while the LUMO comes mainly from the antibonding of p_z orbitals between N_m and N_p. Meanwhile, the bader charge analysis reveals the fact of electron abundant N_4 units and electron deficient Fe atoms (the less electronegative Fe loses 1.67 electrons per atom, and N_p directly bonded to Fe obtains 1.13 electrons per atom, while the N_m atom remains almost neutral). Such unoccupied antibonding orbitals between N_m and N_p can minimize the influence of excess electrons, which can explain why the $P6_3/mcm$ structure with the N_4 unit is fairly stable.

To probe the electronic structures of the $P6_3/mcm$ structure, we calculated the band structure and density of states (DOS), finding that it exhibit metallic features. A comparison of the band structures of FeN_2, Fe_0N_2 (all Fe atoms removed out of the lattice and a uniform compensated background charge (8e/Fe) is applied to preserve the total valence electrons of the system) is performed (Fig. 4a). The difference between the resultant band structure of a hypothetical Fe_0N_2 system (red dash lines) with the realistic one of FeN_2 indicates that the Fe atoms not only act as electron donors but also bond with N. As shown in Fig. 4b, the DOS reveal that the Fe-*d* and N-*p* states are energetically degenerate in the valence bands region, which facilitates the Fe−N hybridization and the formation of covalent bond. These results offer further support for the ionic and covalent bonding nature of Fe-N bonds as described above. We noted that the large bands crosses the E_f and the bands appears "flat band-steep band" characteristic[50] around the E_f. These are typical features favorable for strong EPC and superconductors. Using the linear response theory, we calculated the phonon DOS (PHDOS), Eliashberg function $\alpha^2F(\omega)$ and the strength of the e-ph coupling $\lambda(\omega)$ of the $P6_3/mcm$ structure (Fig. 4c). The Eliashberg function integrates to a $\lambda = 0.62$ and gives the logarithmic average ~400 cm^{-1}, being much closer to the *oP*10-FeB_4 value of ~430 cm^{-1}. The main contributor to the EPC originates from the mixed Fe-N modes below 1000 cm^{-1} (85% of λ) and the high-frequency vibrations from N_4 units (15% of λ) (Fig. 4d). Using the Allen-Dynes equation[51], with the calculated ω_{log} of 643 K and typical $\mu^* = 0.1$~0.15, it reveals that the $P6_3/mcm$ structure is a weak-coupling BCS-type superconductor with a superconducting T_c of 4~8 K. Moreover, the most commonly known transition-metal pernitrides crystallize can act as hard materials, such as MnN_2 ($H_V = 19.9$ GPa), CoN_2 (16.5 GPa), and NiN_2 (15.7 GPa)[52]. Fe in

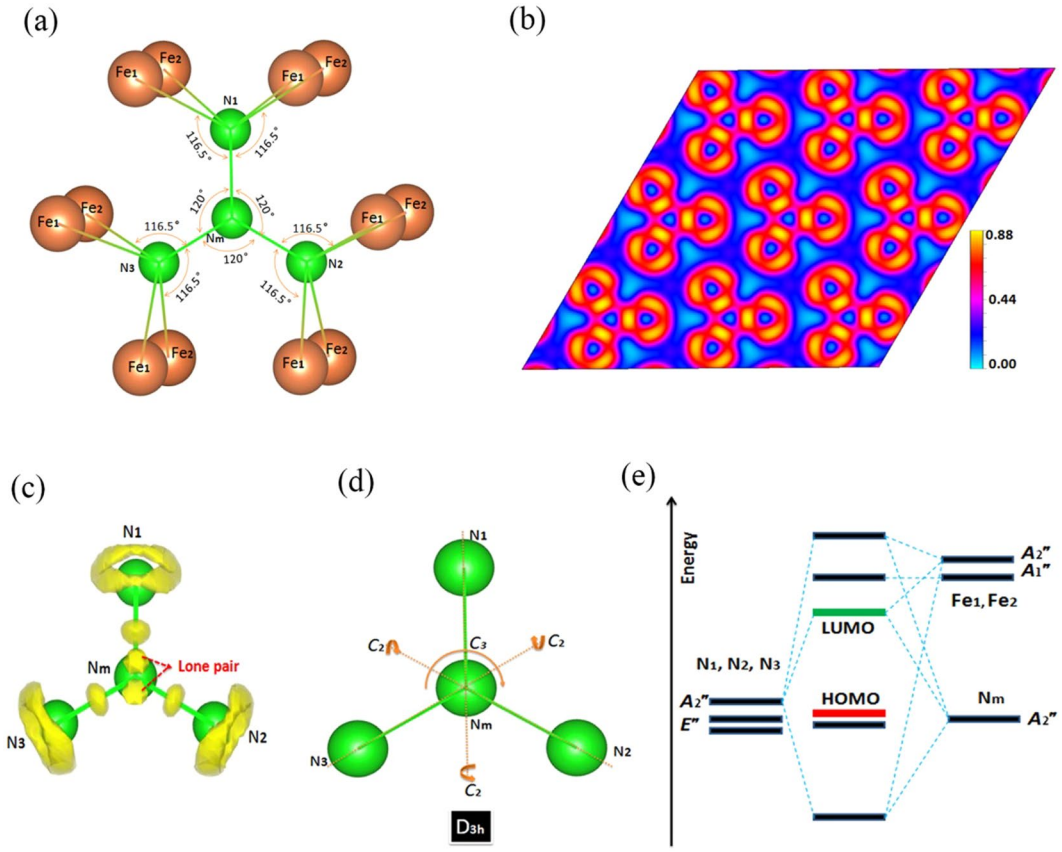

Figure 3. (**a**) The structural feature of N_4 unit with Fe in the $P6_3/mcm$-FeN_2. (**b**) The ELF plots (001) of $P6_3/mcm$ structure at 250 GPa with an isosurface value of 0.75. (**c**) The ELF plots of N_4 unit in the $P6_3/mcm$ structure at 250 GPa. (**d**) The atomic model for hypothetic N_4 cluster with typical symmetry operations marked out. (**e**) The orbital interaction diagram of a N_4 unit with Fe atom.

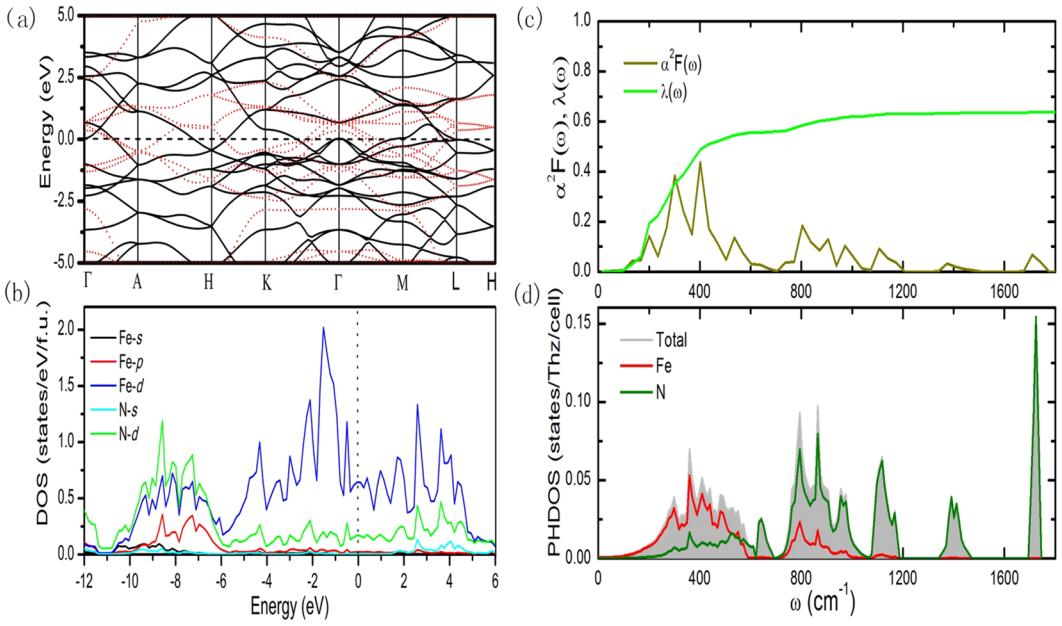

Figure 4. (**a**) Electronic band structure and (**b**) the projected density of states for $P6_3/mcm$-FeN_2 structure at 250 GPa, the red dash lines represent the band structure of the N sublattice with a uniform compensated background. (**c**) The calculated Eliashberg EPC spectral function $\alpha^2F(\omega)$ and its integral $\lambda(\omega)$ and (**d**) the projected phonon density of states for $P6_3/mcm$-FeN_2 structure at 250 GPa.

the same period as Mn, Co and Ni and the $P6_3/mcm$-FeN_2 phase is as a typical transition-metal pernitride, so the $P6_3/mcm$-FeN_2 is also regarded as hard material here. We calculated and obtained its mechanical properties including bulk modulus B (341 GPa), shear modulus G (247 GPa), young's modulus Y_m (597 GPa), and Vicker's hardness ($H_V = 29$ GPa) at ordinary pressure. As expect, the result shows that the $P6_3/mcm$-FeN_2 phase exhibits highly incompressible. Bases on a correlation the covalent bond with hardness, we attribute the excellent mechanical properties of this structure to the N_4 units with strong covalent bonds dominantly by providing coulomb repulsion between the nitrogen atoms as a result of charge transfer from Fe.

Conclusion

Using a structure search method based on CALYPSO methodology and density functional total energy calculations, we systematically studied the phase stabilities and the structures of Fe-N systems in the N-rich regime. We identify two stoichiometric FeN_4 and FeN_2 compounds with unexpected structures that might be experimentally synthesizable under pressure. At 1:4 composition, the energetically favored structure stabilizes in a low *P*-1 symmetry at low pressure and adopts a high symmetric orthorhombic *Cmmm* structure at high pressure, both having a infinite 1D linear nitrogen chains. Differently, the *Cmmm* phase has Fe 8-coordination decahedrons, in contrast with Fe 6-coordination in the octahedrons of *P*-1 structure. At 1:2 composition, an unknown energetically favored hexagonal $P6_3/mcm$ structure was firstly discovered at above 228 GPa. Structurally, it is intriguing with the appearance of exotic triadius-like N_4 unit. In the N_4 unit, the N_m atom possesses one lone pair of electrons at its p_z orbital and forms three N = N covalent bonds with peripheral N_p atoms, owing to its sp^2 hybridization. To probe the electronic structures of the $P6_3/mcm$ structure, it reveals that its intriguing feature gives rise to a set of remarkable properties with an unexpectedly T_c of 4~8 K and a good mechanical property.

References

1. Zhou, R. & Zeng, X. C. Polymorphic Phases of sp3-Hybridized Carbon under Cold Compression. *J. Am. Chem. Soc.* **134**, 7530–7538 (2012).
2. Tornieporth-Oetting, I. C. & Klapotke, T. M. Covalent Inorganic Azides. *Angew. Chem. Int. Ed.* **34**, 511 (1995).
3. Hansen, N. & Wodtke, A. M. Velocity Map Ion Imaging of Chlorine Azide Photolysis: Evidence for Photolytic Production of Cyclic-N_3. *J. Phys. Chem. A.* **107**, 10608–10614 (2003).
4. Larson, C. *et al*. Observation of Photochemical C−N Bond Cleavage in CH_3N_3: A New Photochemical Route to Cyclic N_3. *J. Phys. Chem. A* **112**, 1105–1111 (2008).
5. Cacase, F., Petris, G. & Troiani, A. Experimental Detection of Tetranitrogen. *Science* **295**, 480–481 (2002).
6. Vij, A., Pavlovich, J. G., Wilson, W. W., Vij, V. & Christe, K. O. Experimental Detection of the Pentaazacyclopentadienide (Pentazolate) Anion, cyclo-N^{5-}. *Angew. Chem., Int. Ed.* **41**, 3051–3054 (2002).
7. Christe, K. O., Wilson, W. W., Sheehy, J. A. & Boatz, J. A. N^{5+}: A Novel Homoleptic Polynitrogen Ion as a High Energy Density Material. *Angew. Chem., Int. Ed.* **38**, 2004–2009 (1999).
8. Vij, A. *et al*. Polynitrogen Chemistry. Synthesis, Characterization, and Crystal Structure of Surprisingly Stable Fluoroantimonate Salts of N^{5+}. *J. Am. Chem. Soc.* **123**, 6308–6313 (2001).
9. Jeremy, M. S. & Deepak, S. The structure and reactivity of iron nitride complexes. *Dalton Trans.* **41**, 1423–1429 (2012).
10. Suzuki, K., Morita, H., Kaneko, T., Yoshida, H. & Fujimori, H. Crystal structure and magnetic properties of the compound FeN. *J. Alloys. Compd.* **201**, 11 (1993).
11. Wessel, M. & Dronskowski, R. A New Phase in the Binary Iron Nitrogen System?—The Prediction of Iron Pernitride, FeN_2. *Chem. Eur. J.* **17**, 2598 (2011).
12. Wang, Z. *et al*. Prediction and characterization of the marcasite phase of iron pernitride under high pressure. *J. Alloys. Compd.* **702**, 132 (2017).
13. Vandenberg, J. M. & Matthias, B. T. Superconductivity and structural behavior of hexagonal MoN and related Mo compounds. *Mater. Res. Bull.* **9**, 1085–9 (1974).
14. Medvedev, S. A. *et al*. Phase stability of lithium azide at pressures up to 60 GPa. *J. Phys.: Condens. Matter.* **21**, 195404 (2009).
15. Wang, H. *et al*. Ultra-incompressible phases of tungsten dinitride predicted from first principles. *Phys Rev B.* **79**, 132109 (2009).
16. Peng, F., Wang, Y., Wang, H., Zhang, Y. & Ma, Y. Stable xenon nitride at high pressures. *Phys Rev B.* **92**, 094104 (2015).
17. Peng, F., Yun, H., Liu, H. & Yao, Y. Exotic stable cesium polynitrides at high pressure. *Scientific Reports.* **5**, 16902 (2015).
18. Wang, Y., Lv, J., Zhu, L. & Ma, Y. Crystal structure prediction via particle-swarm optimization. *Phys. Rev. B* **82**, 094116 (2010).
19. Wang, H., Tse, J. S., Tanaka, K., Iitaka, T. & Ma, Y. Superconductive sodalite-like clathrate calcium hydride at high pressures. *Proc. Natl. Acad. Sci. USA* **109**, 6463–6466 (2012).
20. Peng, F., Miao, M., Wang, H., Li, Q. & Ma, Y. Predicted Lithium–Boron Compounds under High Pressure. *J. Am. Chem. Soc.* **134**, 18599–18605 (2012).
21. Li, Y., Feng, X., Liu, H. *et al*. Route to high-energy density polymeric nitrogen t-N via He− N compounds. *Nat. Commun.* **9**, 722 (2018)
22. Zhu, L. *et al*. Substitutional Alloy of Bi and Te at High Pressure. *Phys. Rev. Lett.* **106**, 145501 (2011).
23. Nishio-Hamane, D., Zhang, M., Yagi, T. & Ma, Y. High-pressure and high-temperature phase transitions in $FeTiO_3$ and a new dens-$FeTi_3O_7$ structure. *Am. Mineral.* **97**, 568–572 (2012).
24. Guillaume, C. *et al*. Cold melting and solid structures of dense lithium. *Nat. Phys.* **7**, 211–214 (2011).
25. Zhu, L. *et al*. Reactions of xenon with iron and nickel are predicted in the Earth's inner core. *Nat. Chem.* **6**, 644–648 (2014).
26. Chen, Y. *et al*. High-pressure phase transitions and structures of topological insulator BiTeI. *J. Phys. Chem. C.* **117**, 25677–25683 (2013).
27. Chen, Y. *et al*. Exploring high-pressure lithium beryllium hydrides: a new chemical perspective. *J. Phys. Chem. C.* **117**, 13879–13886 (2013).
28. Zhong, X. *et al*. Tellurium hydrides at high pressures: High-temperature superconductors. *Phys. Rev. Lett.* **116**, 057002 (2016).
29. Li, Y. *et al*. Metallic icosahedron phase of sodium at terapascal pressures. *Phys. Rev. Lett.* **114**, 125501 (2015).
30. Li, Y., Hao, J., Liu, H., Li, Y. & Ma, Y. The metallization and superconductivity of dense hydrogen sulfide. *J. Chem. Phys.* **140**, 174712 (2014).
31. Blöchl, P. E. Projector augmented-wave method. *Phys. Rev. B* **50**, 17953–17979 (1994).
32. Kresse, G. & Joubert, D. From ultrasoft pseudopotentials to the projector augmented-wave method. *Phys. Rev. B* **59**, 1758–1775 (1999).
33. Kresse, G. & Furthmüller, J. Efficient iterative schemes for ab initio total-energy calculations using a plane-wave basis set. *Phys. Rev. B* **54**, 11169 (1996).
34. Monkhorst, H. J. & Pack, J. D. Special points for Brillouin-zone integrations. *Phys. Rev. B* **13**, 5188 (1976).

35. Giannozzi, P. *et al*. QUANTUM ESPRESSO: A modular and open-source software project for quantum simulations of materials. *J Phys: Condens Matter* **21**, 395502 (2009).
36. Parlinski, K., Li, Z. Q. & Kawazoe, Y. First-Principles Determination of the Soft Mode in Cubic ZrO_2. *Phys. Rev. Lett.* **78**, 4063 (1997).
37. Samir, F. M. Chemical bonding and magnetic trends within the iron–nitrogen system. *J. Alloys. Compd.* **345**, 72–76 (2002).
38. Laniel, D. & Dewaele, A. Garbarino, G. High Pressure and High Temperature Synthesis of the Iron Pernitride FeN_2. *Inorganic chemistry* **57**, 6245 (2018).
39. Prasad, D. L. V. K., Ashcroft, N. W. & Hoffmann, R. Evolving Structural Diversity and Metallicity in Compressed Lithium Azide. *J. Phys. Chem. C.* **117**, 20838–20846 (2013).
40. Zhu, H. *et al*. Pressure-induced series of phase transitions in sodium azide. *J. Appl. Phys.* **113**, 033511 (2013).
41. Wang, X., Li, J., Zhu, H., Chen, L. & Lin, H. Polymerization of nitrogen in cesium azide under modest pressure. *J. Chem. Phys.* **141**, 044717 (2014).
42. Patra, A. K. *et al*. Stable Eight-Coordinate Iron (III/II) Complexes. *Inorg. Chem.* **49**, 2032–2034 (2010).
43. Seredyuk, M. *et al*. Homoleptic Iron (II) Complexes with the Ionogenic Ligand 6,6′-Bis(1H-tetrazol-5-yl)-2,2′-bipyridine: Spin Crossover Behavior in a Singular 2D Spin Crossover Coordination Polymer. *Inorg. Chem.* **54**, 7424–7432 (2015).
44. Diebold, A. & Hagen, K. S. Iron(II) Polyamine Chemistry: Variation of Spin State and Coordination Number in Solid State and Solution with Iron (II) Tris(2-pyridylmethyl)amine Complexes. *Inorg. Chem.* **37**, 215–223 (1998).
45. Bu, X.-H. *et al*. Synthesis, characterization and crystal structures of the cobalt(II) and iron(II) complexes with an octadentate ligand, 1,4,7,10-tetrakis(2-pyridylmethyl)-1,4,7,10-tetraazacyclododecane (L), $[ML]^{2+}$. *Polyhedron*, **19**, 431–435 (2000).
46. Armentano, D. *et al*. A novel supramolecular assembly in an iron(III) compound exhibiting magnetic ordering at 70 K. *Chem. Commun.* **211**, 1160–1161 (2004).
47. Boudalis, A. K. *et al*. A Family of Enneanuclear Iron(II) Single-Molecule Magnets. *Chem. – Eur. J.* **14**, 2514–2526 (2008).
48. Barsukova-Stuckart, M. *et al*. Polyoxopalladates Encapsulating 8-Coordinated Metal Ions, $[MO_8PdII_{12}L_8]n-$ ($M = Sc^{3+}$, Mn^{2+}, Fe^{3+}, Co^{2+}, Ni^{2+}, Cu^{2+}, Zn^{2+}, Lu^{3+}; $L = PhAsO_3^{2-}$, $PhPO_3^{2-}$, SeO_3^{2-}). *Inorg. Chem.* **51**, 13214–13228 (2012).
49. Tsai, F.-T., Lee, Y.-C., Chiang, M.-H. & Liaw, W.-F. Nitrate-to-Nitrite-to-Nitric Oxide Conversion Modulated by Nitrate-Containing $\{Fe(NO)_2\}_9$ Dinitrosyl Iron Complex (DNIC). *Inorg. Chem.* **52**, 464–473 (2013).
50. Simon, A. Superconductivity and Chemistry. *Angew. Chem. Int. Ed.* **36**, 1788 (1997).
51. Allen., P. B., Dynes & Transition, R. C. temperature of strong-coupled superconductors reanalyzed. *Phys. Rev. B.* **12**, 905 (1975).
52. Liu, D., Gall, Z. T. Y. & Khare, S. V. Electronic and bonding analysis of hardness in pyrite-type transition-metal pernitrides. *Phys. Rev. B* **90**, 134102 (2014).

Acknowledgements

This work is supported by the China National Science Foundation (Grant No. 11604270); the Introduce Talents Start Scientific Research Funds of Southwest Jiaotong University (2017 × 05020); the Sichuan Province, Applied Science and Technology Project (Grant No. 2017JY0056); the Fundamental Research Funds for the Central Universities (2017 × 02012, 2018GF08); the Open Research Fund of Computational Physics Key Laboratory of Sichuan Province, Yibin University (No. 2016H01038, 2016Q3001); the Open Research Fund of Province of state key laboratory cultivation base construction, Inner Mongolia University of Science & Technology (No. 2015H01424).

Author Contributions

Yuanzheng Chen wrote the manuscript, Xinyong Cai prepared Figures 1–4. Hongyan Wang, Hongbo Wang, and Hui Wang reviewed the manuscript.

Additional Information

Supplementary information accompanies this paper at https://doi.org/10.1038/s41598-018-29038-w.

Competing Interests: The authors declare no competing interests.

Publisher's note: Springer Nature remains neutral with regard to jurisdictional claims in published maps and institutional affiliations.